Journal of Energy Storage 77 (2024) 109941

Contents lists available at ScienceDirect

Journal of Energy Storage

journal homepage: www.elsevier.com/locate/est

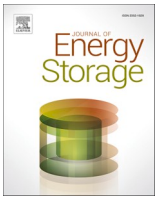

Research papers

Manufacturing cost comparison of tabless vs. standard electrodes for cylindrical lithium-ion batteries

Martin F. Börner [a,b,c,d,*], Ahmad M. Mohsseni [e], Nilava De [a,b,c], Matthias Faber [a,b,c], Florian Krause [a,b,c], Weihan Li [a,b,c], Stephan Bihn [a,b,c], Florian Ringbeck [a,b,c], Dirk Uwe Sauer [a,b,c,d,f]

[a] Chair for Electrochemical Energy Conversion and Storage Systems, Institute for Power Electronics and Electrical Drives (ISEA), RWTH Aachen University, Germany
[b] Jülich Aachen Research Alliance, JARA-Energy, Germany
[c] Center for Ageing, Reliability and Lifetime Prediction of Electrochemical and Power Electronic Systems (CARL), RWTH Aachen University, Germany
[d] Institute for Power Generation and Storage Systems (PGS), E.ON ERC, RWTH Aachen University, Germany
[e] UK Battery Industrialisation Centre, Coventry, United Kingdom
[f] Helmholtz Institute Münster (HI MS), IEK-12, Forschungszentrum Jülich, Germany

ARTICLE INFO

Keywords:
Lithium-ion battery
Manufacturing
Production
Tabless
Electrode
Costs

ABSTRACT

The introduction of the tabless electrode design for lithium-ion battery cells by Tesla in 2020 and its successful industrialisation for the 2022 Model Y marked a significant breakthrough in the realm of cylindrical cell designs for batteries. This innovative approach allowed for larger cell designs while maintaining optimal thermal performance through active cooling on the system level. While prior research has focused on the advantages of this tabless design in terms of thermal management, this work explores a distinct benefit during the electrode manufacturing process. Traditionally, cylindrical battery cells utilize an electrode coating method that leaves gaps on the electrode surface to accommodate tab welding. Consequently, the coating machine operates in an intermittent coating mode, leading to a substantial reduction in achievable coating speed. In contrast, the tabless electrode design enables the continuous deposition of the active material by the coating machine. This advancement results in a remarkable increase in the coating speed, exceeding 60 %, which more than compensates for the additional costs associated with laser cutting the edge of the tabless electrode. This paper demonstrates how the adoption of tabless electrodes in the manufacturing process leads to a considerable cost reduction, from 2.029 to 1.698 €/kWh, while maintaining all other factors constant. Although this cost reduction may appear modest concerning the total cell costs, the cumulative savings at the giga-factory scale become significant, making this advancement economically viable and impactful.

1. Introduction

Over the past years, the trend towards using larger battery cells for electric vehicle battery systems has continued to spread through the industry, with the BYD Blade cell standing out as an extreme example recently [1,2]. These larger cells offer advantages during production, especially during the integration of many battery cells into a battery system for an electric vehicle [3]. Tesla, a prominent player in the electric vehicle market, initially used cylindrical cells in the 18,650 format but quickly transitioned to larger 21,700 cells [4]. In early 2020, Tesla unveiled a patent for a new "tabless" electrode design, which media analysis suggested could improve current distribution and reduce ohmic losses during fast charging [5–7]. Tesla's CEO, Elon Musk, was quick to point out on Twitter that the development was "Way more important than it sounds" and during "Battery Day" later in 2020, Tesla introduced an even larger cell size in the form of the 4680 format [8,9]. This expansion in cell size was made possible by the reduced ohmic resistance and enhanced thermal pathway to external cooling systems facilitated by the tabless design, as further supported by subsequent studies [10].

Our analysis focusses on an additional advantage of tabless cylindrical cell designs, first mentioned by Degen and Krätzig [11], pertaining to the manufacturing of the electrodes. Standard electrodes for cylindrical cells with welded tabs leave gaps in the electrode coating to

* Corresponding author at: Institute for Power Electronics and Electrical Drives (ISEA), RWTH Aachen University, Germany.
E-mail addresses: martin.boerner@isea.rwth-aachen.de, batteries@isea.rwth-aachen.de (M.F. Börner).

https://doi.org/10.1016/j.est.2023.109941
Received 17 August 2023; Received in revised form 9 November 2023; Accepted 1 December 2023
Available online 11 December 2023

weld the tables [12,13]. These gaps are created during the coating process, by retracting the slurry through the fluid delivery system, advancing the current collector foil, and then recommencing the coating process [14]. Consequently, the achievable coating speed is significantly reduced. In contrast, a tabless electrode design eliminates the need for such gaps, leading to a significantly higher coating speed.

This study demonstrates how the battery cell design change to tabless electrodes in cylindrical cell influences the productions costs in a large-scale manufacturing context. A bottom-up cost calculation approach, focussing on the production process changes, allows us to individually study the effects on different cost categories. The suggested model facilitates the analysis of different economic and technical parameters, demonstrated in an analysis of the significance of several parameters. Generalising the results demonstrates the importance of battery and production process design innovations to reduce battery costs. Production output increases have a particularly strong effect on costs when fixed costs, like labour costs, are high.

In the following section, we will compare tabless electrodes to standard electrodes, focusing on features relevant to the applied manufacturing processes. Subsequently, in Section 2.4, we will analyse the production processes of both electrode designs to identify pertinent differences for comparing manufacturing costs. The aim is to evaluate the cost difference between the two processes using the bottom-up method. The conclusion will provide a summary of the study's findings and limitations while suggesting potential areas for future research.

2. Battery design comparison and process considerations

2.1. Standard electrode design

Standard cylindrical cells have electrodes with tabs that are welded to the copper or aluminium electrode foil. This welding process requires leaving gaps in the active material coating due to the presence of the tabs. To ensure a large contact area with the electrode foil, the tabs are welded across the electrode width. In Fig. 1 this is illustrated with a photo of the electrodes of an 18,650 cell from a cell opening performed at ISEA, along with a corresponding drawing of the electrode layout [15]. In this layout, the tab is positioned in the middle of the cathode, and there is additional blank foil at the ends of the electrodes. CT scans of commercial cylindrical battery cells indicate that the tab position can vary from once cell model to another, see Fig. 2. Regardless of the specific tab position and whether there is an additional coating gap to create the blank foil at the ends, every cell will have at least one area of blank foil on each electrode meaning that an intermittent coating process must be performed.

2.2. Tabless electrode design

Tabless electrodes differ from standard electrodes of cylindrical cells in that they do not have tabs welded across them. Instead, the electrical contact between the electrode and the housing is achieved by having the copper or aluminium foil overhang the coated area on the side of the electrode. Tesla refers to these overhangs as "flags", which are then slotted and bent flat with the top and bottom of the jelly roll during winding [17]. The design is reminiscent of the way some (film) capacitors are constructed. Another comparison would be flat wound pouch cells. In those cells the foils edge connects to tabs that are themselves connected to the contact points of the cell enclosure. New to the Tesla design and patent is the slitting of the edge to form the flags that can be bent to form flat contact surfaces on the jelly roll cylinder faces. Fig. 3 provides a visual representation of the cathode side of a partially unwound jelly roll, where the trimmed flags are visible, indicating a likely integration of further slitting or laser trimming steps during the flag creation process.

2.3. Baseline electrodes for this study

This study specifically focuses on the cost difference associated with the production process, rather than the cost improvements that may arise from transitioning to a larger cell format. To maintain consistency, we assume that the electrode length and the coated width of the electrodes are the same for both cell types. The electrode dimensions are derived from measurements of Samsung INR 21700 50E cells, which were disassembled in our laboratory, as shown in Fig. 4. The anode dimensions are slightly larger than the cathode dimensions to achieve a slight anode overhang. Considering that the larger coated area of the anode limits the production output of one pair of anode and cathode coating machines, we consider the anode as the baseline electrode for our subsequent calculations. For the size of the flags, Tesla specifies 3 to 6 mm in their patent [17]. We select 4 mm as a reasonable intermediate value for the 21,700-based cell format. Additionally, since our electrode dimensions are based on the Samsung 50E cell with 18 Wh, we assume

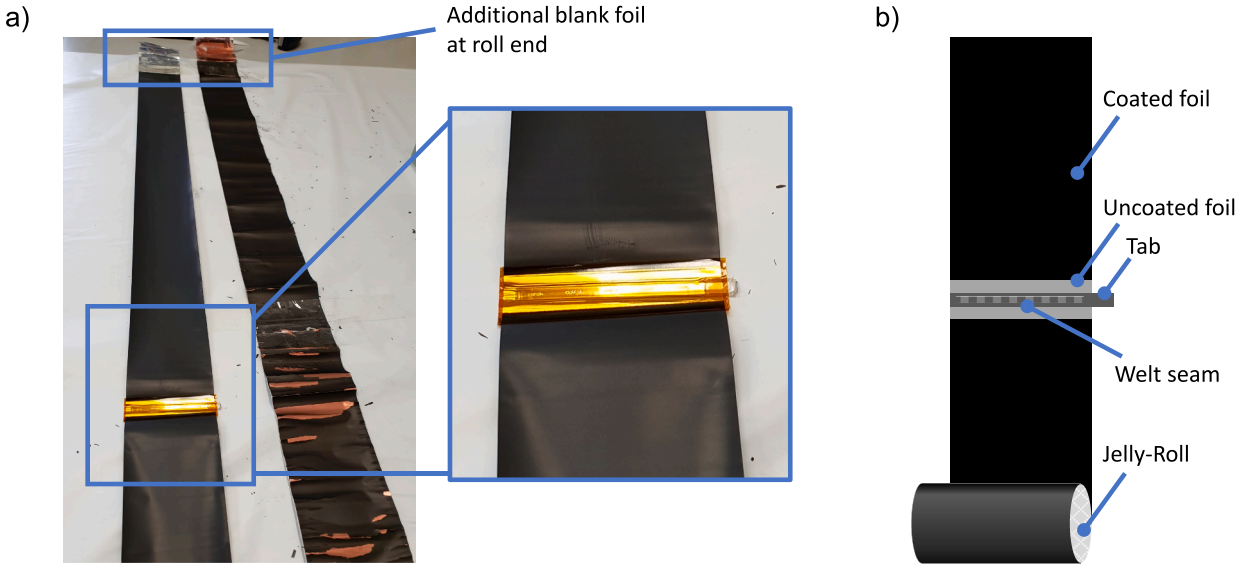

Fig. 1. a) A typical 18,650 cell was opened in the ISEA laboratories. The enlarged portion shows how the coating is interrupted to leave a blank area of foil to weld the tab. The weld seam is covered with tape. b) shows a drawing of the electrode with labels for the individual features.

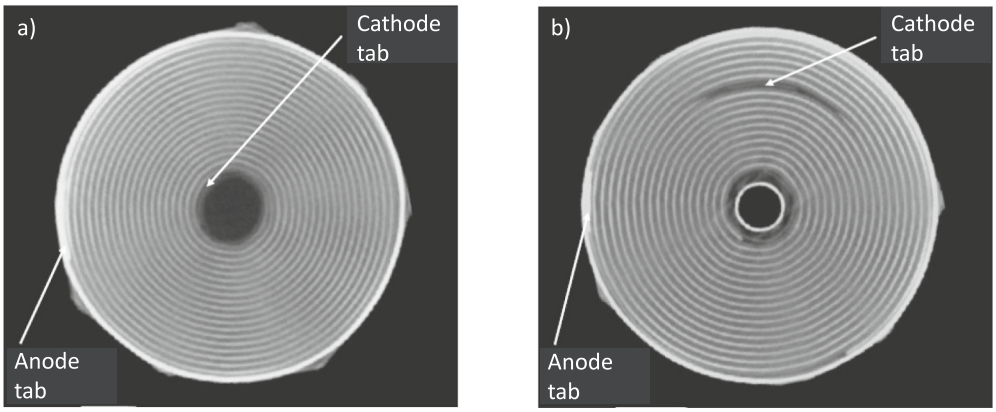

Fig. 2. CT scans of a) an LG 18650 cell and b) a Panasonic 18,650 cell showing the positions of the tables [16].

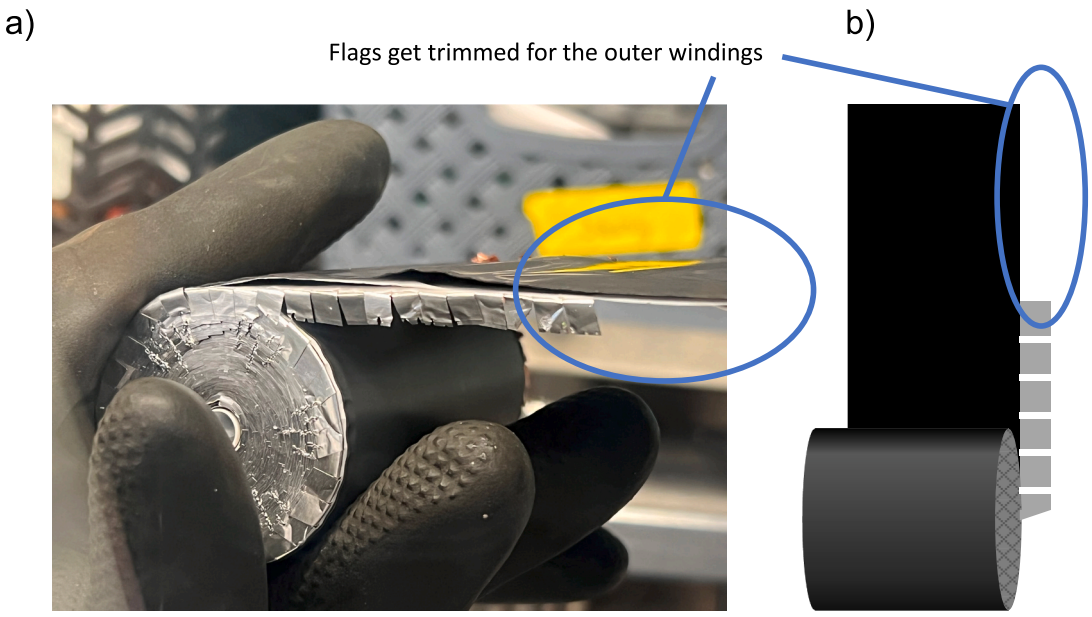

Fig. 3. a) Partially unwound jelly roll of the Tesla 4680 cell with b) a diagram showing how the slotted overhang of the current collector forming the tabs is trimmed off for the outermost winds (Picture of the 4680 jelly-roll a) was shared with us by Dr. Weikang Li, UC San Diego).

that the energy of the two cells in our analysis are 18 Wh [18]. Given that the costs for current collector foils only make up a small proportion of the cell material costs, we assume that the small difference in foil weight and area of approx. 6.15 % is negligible in terms of costs [19,20].

2.4. *Manufacturing process considerations*

To compare the manufacturing costs of the two electrode types, we must carefully consider the changes in the manufacturing process. A significant difference arises from the coating machines' operation mode, where the continuous process allows for higher speeds compared to intermittent process. While very high intermittent coating speeds have been demonstrated in research, one of the largest suppliers of production equipment for lithium-ion battery factories, *Wuxi Lead Intelligent Equipment*, specifies the maximum coating speeds of a large-scale tandem coater in intermittent mode as 60 m/min, whereas it can achieve 100 m/min in continuous mode [21,22]. Intermittent coating faces challenges in achieving a uniform coating thickness at the gaps' edges and creating steep coating edges [23]. Variations in the coating thickness can negatively impact the cell performance, for instance, by compressing the separator or causing an imbalance in anode and cathode active material leading to accelerated ageing due to plating [24,25]. These challenges, along with unwanted vibrations in the coating machine during slot-die movement, limit the coating speed in intermittent mode compared to continuous mode when aiming for the same production quality [26]. This observation was verified in talks with experts from industry and other academic battery production researchers. While the intermittent and continuous coating processes are the subject of ongoing development efforts and numbers will keep on improving, the process speed difference is likely to remain relevant.

When announcing the 4680 cell-format, Tesla also announced moving from a wet coating and drying process to a dry coating process that does not require a separate drying step in a tunnel oven. It is unclear if this process has been successfully implemented in mass production facilities. For the purpose of this study, which focuses on the effect of the tabless electrode design, we assume the same wet coating process for both electrode types and do not consider the requirement of a dry room environment given the active material of our baseline electrodes that are based on the Samsung 50E.

After coating and drying, the evaporated solvents leave the electrode more porous than desired [27]. Therefore, the electrodes are calendered, compressing the active material coating to adjust the porosity [28]. Since the width of the foil is larger than the final electrode width, after calendering the electrode web is separated into multiple webs in a

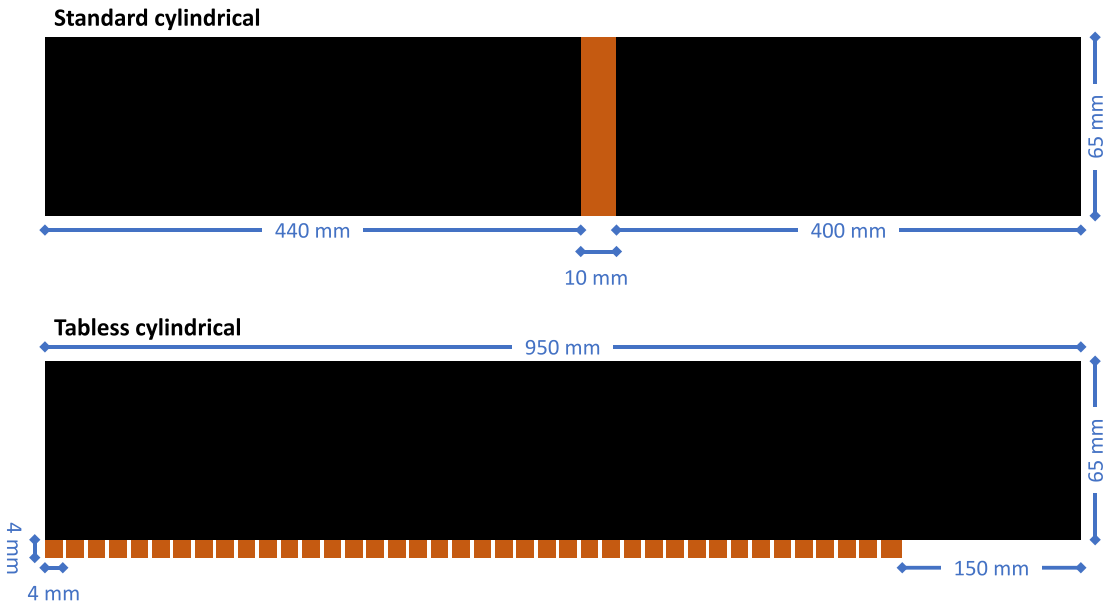

Fig. 4. Dimensions of the evaluated electrodes. The dimensions of the flags are within the dimensions specified by Tesla.

slitting process [28]. Calendering and slitting machines can match the web speeds of the continuous coating process of 100 m/min [11,20]. At low coating speed, one set of calendering and slitting machines has enough throughput to process the output of multiple coating lines. Given that our analysis aims at very large-scale factories, operating multiple coating lines, we assume that the number of calendering and slitting machines can be adapted to the output of the coating and drying lines. Therefore, the increased coating speed of the continuous coating process does not increase the utilisation of the calendering and slitting machines in our model, resulting in no extra cost benefits for the tabless electrode manufacturing.

Following coating, drying, calendering and slitting, the tabless electrode undergoes an additional laser cutting step to form the flags. Tesla's patent describes how bending the flags before winding can be easily achieved using a pair of rollers [17]. Despite being an additional step, it can likely be integrated into the winding machine without significant extra costs. Therefore, we do not factor in additional costs for bending the flags in this study.

Continuing the analysis along the process chain, an additional current collector is welded to the top and bottom of the jelly roll of the tabless cell to facilitate its connection to the cell housing. As this welding step closely resembles the tab welding step in the standard cylindrical cell's production, both in terms of method and the number of welding processes per cell, we have excluded these steps from our analysis of the production process difference. In Fig. 7 the production steps involved in creating the jelly roll for the two cell types are summarised. For our cost breakdown, it suffices to focus on the coating and drying process differences and the additional step of forming the flags of the tabless electrode (Fig. 5).

3. Methodology

3.1. Cost modelling method

Cost analysis methods can be categorised by the approach of estimating the costs: bottom-up or top-down. Top-down cost estimation methods start with the total costs, often of a previous comparable product or process. A differentiation between costs categories or cost centres is based on expert estimations and benchmarking. The top-down approach does not offer detailed insights into the causes of costs in a production facility. However, since it does not require detailed input data, it can be a fast and effective approach during early planning or when analysing the performance of competitors. On the other hand, the bottom-up approach analyses all cost components individually and based on the real cost drivers. Applied to the analysis of manufacturing costs, all cost factors, such as labour, investment and energy costs are evaluated separately for all relevant production processes. This allows for a detailed analysis of the cost structure. For this reason, the model used in this study is based on the bottom-up method. To demonstrate the cost difference between producing electrodes for standard and tabless cells, we can build our bottom-up cost model using different approaches. While many cost models assess battery cell production costs by calculating the required production equipment for a fixed production output per year (usually in GWh) [20,30], this method may result in unused overcapacities caused by the different capacities of the individual machines in the process. In our case, calculating the number of coating

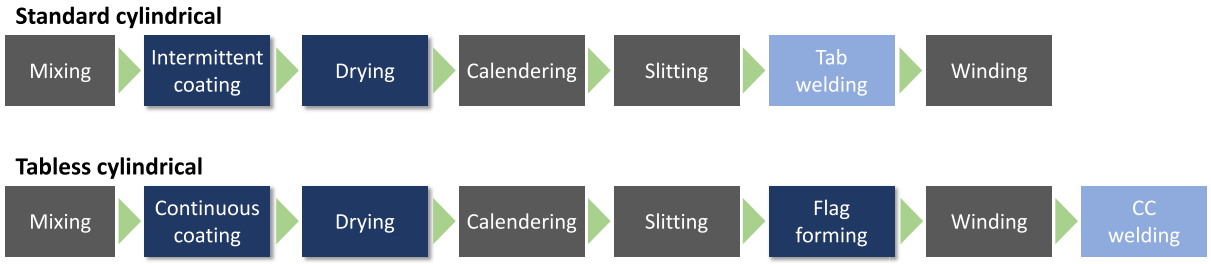

Fig. 5. The manufacturing process steps of creating standard and tabless jellyrolls based on [29]. Process steps that need to be considered to evaluate the cost effects are highlighted in dark blue. (For interpretation of the references to colour in this figure legend, the reader is referred to the web version of this article.)

machines needed for a certain yearly factory output given the difference in output of standard and tabless electrode processes, would result in an uneven equipment utilisation and make the calculated cost difference dependent on the assumes yearly output. Since we are focussing on a specific production step and closely analyse the cost difference, we have chosen to evaluate the costs by calculating the increased productivity of the production equipment affected by the electrode design change, in our case the coating machines. Therefore, we can assume both machines operate at full capacity.

The main difference between the standard and tabless electrode production lies in the possible coating layouts and the resulting coating speeds, along with the additional flag forming process step. The higher coating speed for tabless electrodes enables greater production output for a single machine, leading to the distribution of investment and operation costs over a larger number of cells, and, consequently, reducing costs per kWh. Conversely, the addition of the flag forming process increases the per kWh costs. Evaluating both these factors using the bottom-up method will help us understand the costs implications of producing tabless electrodes.

3.2. Included costs factors

In addition to raw material costs, the main cost factors of a production facility can be categorised into three groups: infrastructure costs for the building and machinery, energy costs and labour costs. Directly attributing the infrastructure costs for machinery can be done by examining the machine investment. Obtaining precise figures for battery production machine costs is challenging due to suppliers' strict non-disclosure agreements. Therefore, we use published values from other costs studies as benchmarks and adjust based on our assumptions.

For the building costs, we base them on the floorspace of the individual machines and add a 100 % markup to account for accessibility around the machine (60 %), materials flow areas (20 %), and storage areas (20 %) [30,31]. This way, the overheads of the factory floorspace are allocated to the production steps based on the machine floorspace. To calculate yearly costs, considering the initial investments in the production infrastructure, we compute the annuities of the investments using an imputed interest rate and assume lifetimes for both machinery and building. Eq. (1) shows how the annual costs of the production infrastructure (C_I) are calculated as the sum of the annuity costs for building and machinery, based on the initial investment (C_b, C_m), their individual lifetimes (n_b, n_m) and the interest rate (r).

$$C_I = C_b \cdot \frac{r}{1-(1+r)^{-n_b}} + C_m \cdot \frac{r}{1-(1+r)^{-n_m}} \quad (1)$$

$$C_M = C_b \cdot m_b + C_m \cdot m_m \quad (2)$$

$$C_E = cons_{el} \cdot c_{el} \quad (3)$$

$$C_L = FTE \cdot PT \cdot c_{WF} \quad (4)$$

$$C_T = C_I + C_M + C_E + C_L \quad (5)$$

$$C_{T,kWh} = \frac{C_T}{OP} \quad (6)$$

In addition to the investment costs, maintenance costs (C_M) for both building and machinery are assumed as a fixed percentage (m_b, m_m) of the initial investment costs per year (Eq. (2)). Energy costs (C_E) can be directly assigned to the production steps by considering the energy consumption of individual machines in kWh ($cons_{el}$) and the assumed price per kWh of electricity (c_{el}) (Eq. (3)). Labour costs (C_L) are determined based on the full-time equivalent number of workers (*FTE*), the total production time per year (*PT*) and the employer costs per work hour (c_{WF}) (Eq. (4)). The total manufacturing costs of a process step are thus defined by Eq. (5). To analyse the costs effects, we have to consider the different production outputs for the process variants. We therefore calculate the resulting production output per year in kWh (*OP*) and determine the costs per kWh ($C_{T,kWh}$) (Eq. (6)). Table 1 gives an overview about the general cost calculation assumptions used in this study.

3.3. Parameterisation of the model

In this section, we describe the properties of the production equipment used for this analysis. Considering the wide selection of suppliers for factory-grade production machines, we based our technical parameters for the coating machine on data provided by *Wuxi Lead Intelligent Equipment*, a major supplier to renowned battery producers like CATL, VW, ACC and Tesla [36]. Their machines serve as a reliable baseline for understanding the machinery capabilities in real-world gigafactories.

3.3.1. Coater

As mentioned earlier, we assume the coating machine can operate at a maximum speed of 100 m/min in continuous mode and 60 m/min in intermittent mode. The machine's maximum coating width is assumed to be 700 mm [11,12]. While broader foil widths of up to 1.5 m exist in the industry, detailed data on those machines, such as energy consumption, is limited. The coating machine we consider is a tandem coater, coating and drying both sides of the electrodes one by one, with the drying ovens stacked on top of each other, reducing the machine's size significantly.

We assume a drying oven length of 1 m per 1 m/min of coating speed, resulting in a constant drying time [12]. Accordingly, the tabless electrode's drying oven length is assumed to be 100 m, and the standard electrode's drying oven length is 60 m. Considering the coating apparatus as well as the coil winding and unwinding, we add a constant 15 m to the machine length for both operation modes, based on a drawing of a tandem coater by the equipment supplier Dürr Systems [37]. This gives a total length of 115 m for the coating machine used for the tabless design and 75 m for the standard electrode coater. The width of the machine is assumed to be 7 m, resulting in a footprint of 805 m^2 for the tabless design and 525 m^2 for the standard electrode coater [11].

Table 1
General costs calculation assumptions.

Parameter	Variable	Value	Unit	Note
Infrastructure costs				
Interest rate	r	2.7	%	Average ECB interest rate in 2022 + 2 % [32]
Lifetime machines	n_m	10	years	Typical value [11]
Lifetime building	n_b	30	years	Typical value [11]
Building investment costs	C_b	2800	€/m^2	Value is for an advanced manufacturing facility [33]
Maintenance machines	m_m	2.5	%	Assumed as a percentage of initial investments per year
Maintenance building	m_b	1	%	Assumed as a percentage of initial investments per year
Energy costs				
Electricity price	c_{el}	0.15	€/kWh	Industrial electricity price in Germany in the first half of 2021 [34]
Labour costs				
Hourly costs	c_{WF}	44	€/h	Employer costs for qualified machinist in Germany [35]
General assumptions				
Production time per year	PT	8760	h/year	365 workdays per year, 24 h production
Overall equipment efficiency	OEE	80	%	Only affects output, not energy cons. and labour

We obtained values for the investment costs in coating machinery from Heimes et al., ranging from 30 to 57 mil. € to achieve an annual output of 10 GWh [28]. Using the BatPaC 5.0 model, developed by the Argonne National Laboratory, we obtained investment costs of 90 mil. € for the cathode and 78 mil. € for the anode coaters in a 50 GWh plant, accounting for the solvent recovery needed for the cathode coating machines [20]. The total of 168 mil. $ results in an investment of 3.36 mil. $ per GWh/a, aligning well on the lower side of the range given by Heimes. The coater described in the BatPaC model operates with a coating speed of 80 m/min. Based on the data from the BatPaC manual, we assume that 5 coaters are needed per electrode to achieve the output of 50 GWh/a, with costs of 18 mil. $ for the cathode and 15.6 mil. $ for the anode coater. In an earlier study by Heimes et al., the coating and drying processes were analysed separately, with equal costs assumed for both the coating and the drying machines [40]. However, in our analysis, we use the cost value provided in the BatPaC 5.0 model for the baseline machine operating at 80 m/min with a dryer length of 80 m. To adjust the costs for our coaters with 60 and 100 m dryers, we utilize Eq. (7) for the calculations. This approach yields the cost estimates for our coating and drying machine, as shown in Table 2.

$$C_{m,coater} = \frac{C_{m,BatBaC}}{2} \cdot \left(1 + \frac{L_d}{80\,m}\right) \tag{7}$$

A coating machine's energy consumption, particularly during the drying process, can be substantial. While both natural gas and electricity-powered drying units are available in the market., we believe that electricity powered dryers will be more relevant in future factories due to rising gas prices, supply uncertainties, and the goal of achieving climate neutrality among battery producers. Based on the detailed information from the UKBIC cell production line, we have chosen electrical drying for this study.

In the drying process, most of the energy is used for heating the air in the oven and, in case of the cathode, for solvent recovery from the hot exhaust air. As a result, the energy consumption scales almost linearly with the length of the dryer [42]. Drawing from the Gigafactory Scale analysis in the UKBIC study, which considered a 30 m drying oven with an electricity consumption of 529 kW, we assume that the 60 m and 100 m ovens will consume 1058 kW and 1763 kW for the anode, respectively. For the cathode side, we add 30 % for solvent recovery, resulting in electricity consumption of 1375 kW and 2292 kW for the 60 m and 100 m ovens, respectively [12,42].

Regarding labour requirements, according to BatPaC 5.0, 1.5 workers are needed to operate one machines [20]. To account for logistics tasks, we assume an additional 0.5 workers per machine, bringing the total to 2 workers per machine. These values are assumed for both the cathode and anode coating machines.

3.3.2. Flag forming

As discussed earlier, to manufacture tabless cells an additional process step must be taken into account: forming the flags on the side of the tabless electrode. The flags are created by slitting into the uncoated electrode foil perpendicular to the winding direction. Additionally, the uncoated foil is trimmed at the end of the electrodes (see Fig. 3). To perform the cutting operation, there are several process alternatives, mainly mechanical methods, such as rotary cutting blades, or laser cutting. Laser cutting offers the advantage of combining flag forming and overhang trimming within a single step. Laser cutting machines can achieve cutting speeds for foil notching of 4–6 m/s or 240–360 m/min [43].

Our assumption regarding the flag geometry is that one 4 mm cut is made every 4 mm and the last 150 mm of the overhanging foil is trimmed along the length of the electrode. This means the total cutting length is equivalent to the electrode length. Even with time added for handling, one laser cutting machine can keep up with the line speed of 100 m/min, making it possible to integrate the machine in line with either the slitting or the winding machine. For our calculations, we assume that laser cutting is integrated directly after the slitting process, requiring one laser cutting machine per daughter roll, or one machine per parallelly coated electrode. The integration is done in a way that does not incur additional costs for precision unwinding and winding devices. Therefore, we only consider the costs of the laser cutting unit itself, estimated at 50.000 €, which is approximately two times the cost of the required laser source [44,45].

The electricity consumption of the laser cutting machine is assumed to be under 0.5 kW, making it insignificant compared to the energy consumption of the drying unit [45]. The increase in the machine footprint resulting from the integration of the laser cutter is negligible and will not be considered in further calculations. Moreover, no additional machine operators are required, and since there is no manual loading or unloading of the coils, there is no need for additional logistics workers.

Table 2
Coating and drying machine costs assumed in this study based on BatPaC 5.0 [20] and scaling with dryer length based on Heimes et al. [40] (1$ = 1€, 2022 [41]).

	Intermittent	BatPaC reference	Continuous
Dryer length L_d	60 m	80 m	100 m
Anode Coating costs	13,650,000 €	15,600,000 €	17,550,000 €
Cathode Coating costs	15,750,000 €	18,000,000 €	20,250,000 €

4. Results

4.1. Calculation of the production output

To determine the cost per kWh of the produced cell for both machines, we calculate the annual production capacity of each machine. The coating machine used for standard electrodes operates at a speed of 60 m/min, resulting in a total coated length of 31,536,000 m per year. To calculate the number of parallelly coated electrodes separated during slitting, we consider the coating width, electrode width and assume an uncoated edge of 10 mm on both sides, enabling 10 electrodes to be coated simultaneously. The top portion of Fig. 6 shows how the individual electrodes are intermittently coated and separated during slitting. Only four simultaneously coated electrodes are shown for clarity. Our assumption for the scrap rates of the coating and all downstream processes is 5 %. This in combination with an Overall Equipment Efficiency (OEE) of 80 % leads to a total production output of the coating process of the standard electrode of 252,288,000 cells per year, corresponding to 4.54 GWh.

The coating machine responsible for the tabless electrode operates at 100 m/min, resulting in a total coated length per year of 52,560,000 m per year. Considering the uncoated gap between the individual electrodes required to form the flags, it is still possible to coat 10 electrodes in parallel. The bottom section of Fig. 6 shows the layout of the tabless electrode coating process. Instead of gaps perpendicularly to the coating direction, gaps are created in parallel to the coating direction, not impacting the coating speed. These gaps are subsequently used to form the flags at the sides of the electrodes. Using the same assumptions for scrap rate, OEE, and cell energy, this process yields tabless electrodes amounting to 420,480,000 cells per year, equivalent to 7.57 GWh.

4.2. Analysis of the cost factors of the baseline case

Based on a lifetime of the machines of 10 years and an interest rate of 2.7 %, the yearly annuity costs of the anode and cathode coating machines in the tabless cell production are 2,026,020 € and 2,337,715 €, equivalent to 0.268 € and 0.309 € per kWh produced, respectively. The flag forming lasers entail a total cost of 500,000 €, resulting in annual expenses of 58,000 € per year, corresponding to 0.007 €/kWh. For the standard cell production, the annual costs are 1,575,793 € and

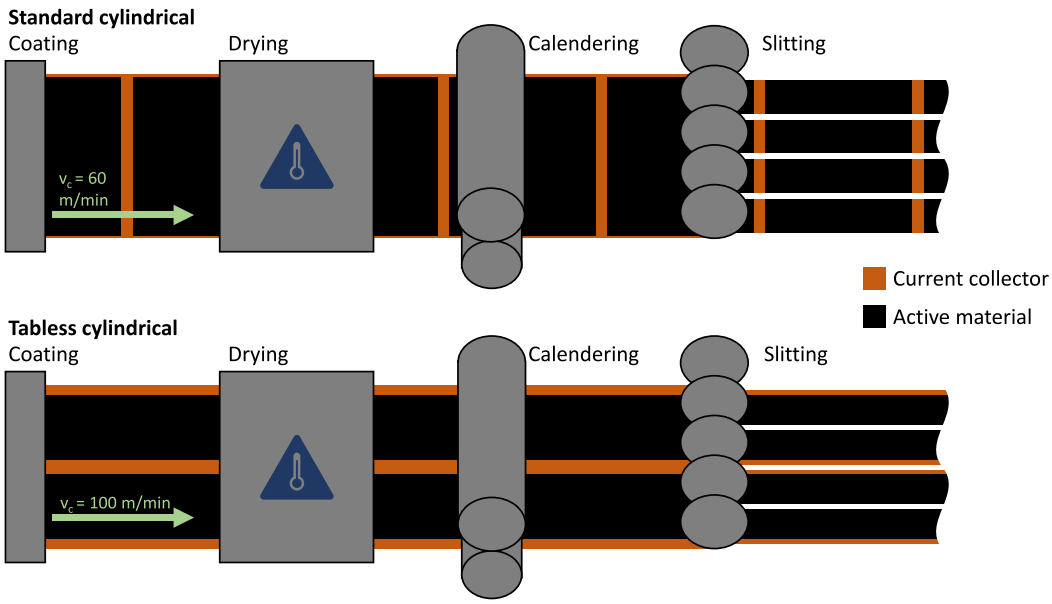

Fig. 6. Electrode production layouts of the electrodes.

1,818,223 €, translating to 0.347 €/kWh and 0.4 €/kWh, respectively.

To calculate the annuity costs of the building, we consider the investment costs based on the total floorspace. The tabless electrode coaters and dryers occupy 3220 m^2, while the standard electrode anode and cathode coaters, including dryers, cover 2100 m^2. This results in building investment costs of 9,016,000 € for the tabless and 5,880,000 € for the standard electrode. Over the building's lifetime of 30 years, the annuity costs are 442,000 € and 288,000 €, which equates to 0.078 €/kWh and 0.094 €/kWh, respectively.

Continuing with infrastructure costs, the yearly maintenance costs for the tabless electrode process amount to 1,060,160 € per year for the anode and cathode machines, or 0.140 €/kWh. For the standard electrode, maintenance costs total 793,800 € per year, resulting in 0.175 €/kWh.

Energy costs are predominantly influenced by electricity expenses of the dryers. The 60 m anode drying oven, with a consumption of 1058 kW, and the cathode process, with solvent recovery, consuming 1375 kW, are assumed for the standard electrode. For the tabless process, the 100 m ovens consume 1763 kW for the anode and 2292 kW for the cathode, including solvent recovery. This leads to total yearly electricity consumption of 21,316,584 kWh and 35,527,640 kWh, respectively. An electricity price of 0.15 €/kWh gives us total yearly costs of 3,197,487 € and 5,329,146 €. Since the production output of the coater and the energy consumption scale linearly with the coating speed or oven length, the costs per kWh produced are 0.306 €/kWh for the anode machines and 0.398 €/kWh for both cathode processes.

Labour costs are the final category considered in our analysis. The increased coating speed and oven length do not impact the number of machine operators. With employer costs for a factory worker in Germany amounting to 44 € per hour, the yearly labour costs for both electrode designs per machine sum up to 770,880 €. The difference in production output leads to costs per kWh produced of 0.102 €/kWh for the tabless and 0.17 €/kWh for the standard electrode, for each coating machine.

The individual cost categories for anode and cathode production of standard and tabless cells are summarised in Table 3. Overall, the production costs of tabless electrodes are 0.331 €/kWh lower compared to standard electrodes, while keeping all other factors constant.

4.3. Sensitivity analysis of selected parameters

To analyse the costs of battery electrode production, certain assumptions about technical and economic parameters were necessary. However, certain factors are location-dependent, while others, like electricity prices and interest rates, can vary due to macro-economic trends and political decisions. In this section, we will perform a sensitivity analysis of key parameters. We have chosen to examine the effects of at least one parameter per cost category. Specially, we will analyse the impact of infrastructure costs for machines and the building by looking at the assumed interest rate and machine costs. For the other two costs categories (energy and labour) we will investigate the impact of the electricity prices and hourly employer labour costs.

Regarding the variation of machine costs, we have set a fixed window of plus and minus 20 % around our baseline assumption. For the other factors, the range of the sensitivity analysis is based on regional or historical variances. We choose one value larger and one value smaller than our base case and marked them on the trendlines of Fig. 7. The interest rate used in our calculation of the infrastructure investment costs will be varied based on historical European Central Bank interest rates between 2008 and 2023. Initially, we added 2 percentage points to the central bank interest rate. To expand the view in our sensitivity analysis, we will add 4 percentage points to the historical maximum value of 4 % and not add any markup to the historical minimum of 0 %, resulting in values of 0 % and 8 % for our analysis [46].

Table 3
Costs breakdown for anode and cathode production and total costs in € per kWh cell produced.

$\frac{€}{kWh}$		Investments		Maintenance	Energy	Labour	Total	
		Machines	Building					
Tabless	Anode	0.275	0.029	0.066	0.306	0.102	0.778	1.698
	Cathode	0.316	0.029	0.074	0.398	0.102	0.920	
Standard	Anode	0.347	0.032	0.082	0.306	0.17	0.936	2.029
	Cathode	0.4	0.032	0.093	0.398	0.17	1.093	

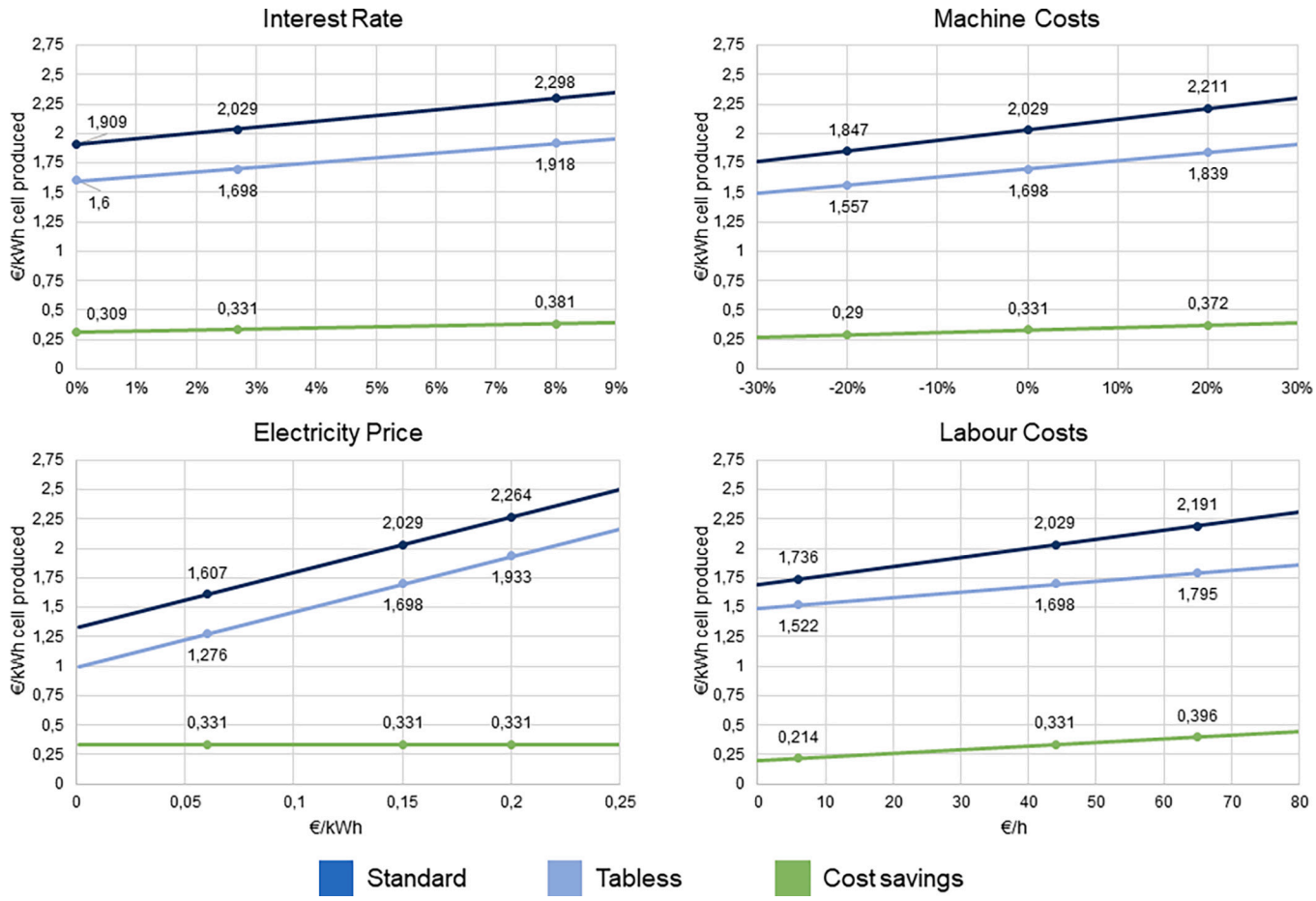

Fig. 7. Sensitivity of selected input factors. Significant points described in the text are marked.

Regarding electricity prices, we can examine either regional variances or historical variances in price. Looking at the historical price variance in Germany between 2008 and 2021, the range is between 0.096 and 0.164 €/kWh, further rising in 2022 to 0.193 €/kWh [34]. Internationally, the lowest industrial electricity prices in 2021 among the members of the International Energy Agency were reported in Finland at 0.071 €/kWh while the highest was reported in the United Kingdom at 0.16 €/kWh [47]. Recently, the German minister for Economic Affairs and Climate Action, Robert Habeck, proposed limiting the industrial electricity price in Germany to 0.06 €/kWh [48]. Based on this data, we will highlight electricity prices of 0.06 and 0.2 €/kWh for analysis.

Labour costs vary significantly from country to country and year to year. Compared to the reported employer costs of 44 €/hour in Germany, labour costs in China, while rising, remain relatively low at about 6 €/hour [49]. On the other hand, a traditionally high-cost country in terms of employer costs is Switzerland at approximately 65 €/hour [50]. In Fig. 7 labour costs of 6 and 65 € per hour are highlighted in addition to our base case.

Rising interest rates and machine costs have an evident impact on the per kWh costs of both electrode designs. However, it is noticeable that the tabless electrode process is somewhat less affected, as the infrastructure costs are spread across a larger production output. In an environment with higher capital costs, focusing on technical innovations to enhance capital utilisation becomes more beneficial. The significant influence of the interest rate on the total costs underscores how market climate, monetary policy decisions, and government incentives, such as low interest loans, can impact the profitability of a production site and influence investment decisions.

Analysing the sensitivity of the production costs to electricity prices reveals a substantial impact on the absolute costs of coating electrodes. In our model, the energy consumption of the drying ovens is the primary determinant of total energy consumption. As the length of the drying oven and the production output are directly linked to the coating speed, we observe that the energy costs per kWh of cell produced are constant. Of course, not only the drying process consumes electricity during coating, so a cost reduction resulting from the increased production output is to be expected but will not be significant in comparison to the overall energy costs.

Labour costs play a pivotal role in determining the total costs of the coating process. Relocating the production of the standard electrode from Germany to China reduces labour costs by approximately 0.294 €/kWh, resulting in potential savings of 14,700,000 € per year for a 50 GWh factory, assuming all the other factors remain constant. With rising labour costs, the impact of the production output improvements in the tabless electrode process becomes even more pronounced. Companies operating in high labour cost environment, especially in Europe and the United States, should prioritize innovations that increase production output per employee to achieve significant cost savings.

5. Discussion

This research successfully demonstrates the substantial cost benefits of transitioning from standard to tabless electrodes for cylindrical battery cell manufacturing. By maintaining all other factors, such as cell format and energy content per cell, constant, our study reveals achievable cost savings of 0.331 €/kWh. These findings indicate that the higher costs associated with the coating machines, building investment, energy consumption and the additional flag forming process can be effectively offset by the significant increase in production output achieved with

tabless electrodes. By focussing specifically on the electrode production and isolating the effects of the design change from other factors, such as larger cell formats and energy density improvements, we gain valuable insights into the cost implications of adopting tabless electrodes. While the objective behind the transition to tabless electrodes centred around enhancing fast charging performance to accommodate the larger 4680 cell format and overcoming challenges in transitioning from wet to dry coating in an intermittent coating process, our study conclusively demonstrates the positive effects of this design change alone on production costs. This is suggesting that even for smaller cells, like the 21,700 format that our baseline electrodes are based on, adopting tabless electrodes can be highly beneficial. In case of the tabless electrodes, technical improvements of the cell design are in line with production cost reductions. This will not always be the case. Battery designers, aiming to reduce costs should therefore always consider the implications of their suggested changes on the production process, to make optimal design decisions. A study by Duffner et al. on general influences of production process optimisations on battery manufacturing costs has shown larger cost effects of an increase in coating speed but used a lower baseline speed of 25 m/min and did not consider the additional flag forming step needed to produce tabless electrodes and the increased energy consumption during drying [51]. Additionally, their study assumes that the coating, drying, calendering and slitting processes are linked. Based on this assumption, at 25 m/min the calendering and slitting processes run at only 25 % of their maximum capability, resulting in a significant reduction of the costs per kWh of those processes when increasing the coating speed to 100 m/min. As described in Section 2.4, our assumptions for large scale battery cell factories are different in that aspect, explaining another part of the difference in our results.

Analysing the individual cost factors and their influence on the total cost savings separately allows us to identify that production locations with high labour costs, like Europe or the US, benefit most from the change to tabless electrodes. A finding that can be generalised to other innovations in productivity. The strong effect of the assumed interest rates and machine costs on total cost savings shows that government incentives, like low interest capital provision, and macro-economic trends can have a significant influence on the competitiveness of a production facility or location.

Since our analysis is limited to the electrode manufacturing costs, especially the coating processes, we did not account for the positive effects tabless electrodes might have on cell lifetime and total cost of ownership in battery system. The values derived in this study, therefore, serve as a conservative lower boundary for the cost effects in real world applications. The improved thermal performance of tabless designs can positively impact system-level costs, allowing for potential downsizing of thermal management systems and increased cell lifetime due to reduced thermal gradients. Consequently, this leads to less need to oversize battery systems to compensate for capacity losses, further reducing system-level costs.

6. Conclusion

Tabless electrode designs offer a significant advantage over standard electrode designs in cylindrical cells by enabling a continuous coating process during electrode production. The associated increase in coating speed results in cost saving of 0.331 €/kWh, offsetting the higher investment costs and the increased energy consumption caused by the longer drying tunnel needed at higher web speeds. Our analysis of the electrodes' features and the required modifications to the production process identified an additional production step necessary for forming the flags at the side of the tabless electrode. The additional costs associated with this process step are included in the cost calculations. The bottom-up analysis of different cost factors allowed us to study under what circumstances the change towards tabless electrodes is most beneficial. While the tabless and standard electrode production process benefited equally from reductions in energy price or consumption, high labour, investment, or interest costs increase the costs reductions resulting from the change to tabless electrodes. Because we analysed the cost effects of the change to tabless electrodes, while keeping all other factors constant, we were able to show that tabless electrodes present advantages even without the benefits that stem from enabling a larger cell format. Independently from Tesla's move to the 4680 cell-format, manufacturers of 21,700 and smaller cells should consider adopting tabless electrodes, or variations of this design in their products. The analysis demonstrates how production cost evaluations can be beneficial during the cell development process in finding cost optimal improvements.

CRediT authorship contribution statement

Martin F. Börner: Conceptualization, Supervision, Investigation, Writing – original draft, Writing – review & editing. **Ahmad M. Mohsseni:** Conceptualization, Investigation, Writing – review & editing. **Nilava De:** Investigation, Writing – review & editing. **Matthias Faber:** Investigation, Writing – review & editing. **Florian Krause:** Writing – review & editing. **Weihan Li:** Conceptualization, Writing – review & editing. **Stephan Bihn:** Funding acquisition, Writing – review & editing. **Florian Ringbeck:** Funding acquisition, Supervision, Writing – review & editing. **Dirk Uwe Sauer:** Conceptualization, Funding acquisition, Supervision.

Declaration of competing interest

The authors declare that they have no known competing financial interests or personal relationships that could have appeared to influence the work reported in this paper.

Data availability

No data was used for the research described in the article.

Acknowledgments

The project "Model2life" on which this publication is based was funded by the German Federal Ministry of Education and Research (BMBF) within the Competence Cluster Battery Utilisation Concepts (BattNutzung) under the grant number 03XP0334. We also thank Dr. Weikang Li from the University of California San Diego for sharing photos from a teardown of a Tesla 4680 cell.

Inclusion and diversity

We support inclusive, diverse, and equitable conduct of research.

References

[1] BYD USA, BYD's New Blade Battery Set to Redefine EV Safety Standards - BYD USA. https://en.byd.com/news/byds-new-blade-battery-set-to-redefine-ev-safety-standards/, 2023.
[2] S. Link, C. Neef, T. Wicke, Trends in automotive battery cell design: a statistical analysis of empirical data, Batteries 9 (2023) 261, https://doi.org/10.3390/batteries9050261.
[3] S. Michaelis, J. Schütrumpf, A. Kampker, H. Heimes, B. Dorn, S. Wennemar, A. Scheibe, S. Wolf, M. Smulka, B. Ingendoh, A. Thielmann, C. Neef, T. Wicke, L. Weymann, T. Hettesheimer, A. Kwade, L. Gottschalk, C. von Boeselager, S. Blömeke, A. Diener, M.-W. von Horstig, J. Husmann, M. Kouli, M. Mund, G. Ventura Silva, M. Weber, M. Podbreznik, A. Schmetz, Roadmap Battery Production Equipment 2030. Update 2023, VDMA Verlag, 2023.
[4] Tesla, Battery Cell Production Begins at the Gigafactory. https://www.tesla.com/blog/battery-cell-production-begins-gigafactory, 2023 (accessed 10 June 2023).
[5] Kunio Tsurata, Mikel Dermer, Rajeev Dhiman WO2020096973A1, 2020.
[6] T. Vincent, The Tesla Tabless Electrode Battery Breakthrough. https://medium.com/0xmachina/the-tesla-tabless-electrode-battery-breakthrough-8f032fb67b81, 2020. (Accessed 10 June 2023).

[7] C. Delbert, Elon Musk: Tesla's Battery Cell Patent Is 'Way More Important Than It Sounds'. https://www.popularmechanics.com/science/a32433420/elon-musk-tesla-battery-cell-patent/, 2020 (accessed 10 June 2023).

[8] Elon Musk, "@EvaFoxU @Tesla Way more important than it sounds" / Twitter. https://twitter.com/elonmusk/status/1258510752396144640, 2020 (accessed 10 June 2023).

[9] Tesla, Annual Meeting of Stockholders and Battery Day | Tesla, 2020. https://www.tesla.com/de_de/2020shareholdermeeting, 2020 (accessed 10 June 2023).

[10] H. Pegel, D. Wycisk, D.U. Sauer, Influence of cell dimensions and housing material on the energy density and fast-charging performance of tabless cylindrical lithium-ion cells, Energy Storage Materials 60 (2023), 102796, https://doi.org/10.1016/j.ensm.2023.102796.

[11] F. Degen, O. Krätzig, Modeling large-scale manufacturing of lithium-ion battery cells: impact of new technologies on production economics, IEEE Trans. Eng. Manage. (2023) 1–17, https://doi.org/10.1109/TEM.2023.3264294.

[12] A. Mohsseni, C. Harper, Pathways to Reduce Energy Consumption in lithium-Ion Battery Cell Manufacturing: A UK Battery Industrialisation Centre Case Study, 2022.

[13] S. Spiegel, T. Heckmann, A. Altvater, R. Diehm, P. Scharfer, W. Schabel, Investigation of edge formation during the coating process of Li-ion battery electrodes, J. Coat. Technol. Res. 19 (2022) 121–130, https://doi.org/10.1007/s11998-021-00521-w.

[14] R. Diehm, H. Weinmann, J. Kumberg, M. Schmitt, J. Fleischer, P. Scharfer, W. Schabel, Edge formation in high-speed intermittent slot-die coating of disruptively stacked thick battery electrodes, Energ. Technol. 8 (2020) 1900137, https://doi.org/10.1002/ente.201900137.

[15] C. Rahe, Untersuchung von Batterieelektroden mit optischen Verfahren, RWTH Aachen University, 2022.

[16] L.K. Willenberg, Volume Expansion and its Effects on the Ageing of a Cylindrical lithium-Ion Battery, RWTH Aachen University, 2020.

[17] B. Eggleston, M. Moors, A. Kalt, M. Grossman, D. Macnaughton, D. Schafer, WO/2022/061187, 2021.

[18] Batemo, INR21700-50E. https://www.batemo.de/products/batemo-cell-library/samsung-inr21700-50e/#get-data-popup, 2022 (accessed 22 June 2023).

[19] M. Greenwood, M. Wentker, J. Leker, A bottom-up performance and cost assessment of lithium-ion battery pouch cells utilizing nickel-rich cathode active materials and silicon-graphite composite anodes, J. Power Sources Adv. 9 (2021), 100055, https://doi.org/10.1016/j.powera.2021.100055.

[20] K.W. Knehr, J.J. Kubal, P.A. Nelson, S. Ahmed, Battery Performance and Cost Modeling for Electric-Drive Vehicles, fifth ed., 2022.

[21] I. Oberdorf, KIT - World's Fastest Manufacture of Battery Electrodes. https://www.kit.edu/kit/english/pi_2014_15826.php, 2014.

[22] Wuxi Lead Intelligent Equipment Co., LTD., Turnkey Solution for LIB Intelligent Manufacturing, 2022.

[23] M. Schmitt, P. Scharfer, W. Schabel, Slot die coating of lithium-ion battery electrodes: investigations on edge effect issues for stripe and pattern coatings, J. Coat. Technol. Res. 11 (2014) 57–63, https://doi.org/10.1007/s11998-013-9498-y.

[24] X. Lin, K. Khosravinia, X. Hu, J. Li, W. Lu, Lithium plating mechanism, detection, and mitigation in lithium-ion batteries, Prog. Energy Combust. Sci. 87 (2021), 100953, https://doi.org/10.1016/j.pecs.2021.100953.

[25] J. Cannarella, C.B. Arnold, The effects of defects on localized plating in lithium-ion batteries, J. Electrochem. Soc. 162 (2015) A1365–A1373, https://doi.org/10.1149/2.1051507jes.

[26] S. Diehm, V. Bravo, M. Gracia, Slot Die Coating of Li-Ion Battery Electrodes. https://www.tvt.kit.edu/338_1103.php#EN, 2014 (accessed 10 June 2023).

[27] D. Schreiner, M. Oguntke, T. Günther, G. Reinhart, Modelling of the Calendering Process of NMC-622 Cathodes in Battery Production Analyzing Machine/Material–Process–Structure Correlations, Energy Technology, 2019.

[28] H.H. Heimes, S. Wennemar, A. Kampker, C. Lienemann, M. Locke, C. Offermanns, S. Michaelis, E. Rahimzei, Production Process of a Lithium-Ion Battery Cell. https://www.pem.rwth-aachen.de/global/show_document.asp?id=aaaaaaaaabdqbtk, 2023 (accessed 10 June 2023).

[29] A. Kwade, W. Haselrieder, R. Leithoff, A. Modlinger, F. Dietrich, K. Droeder, Current status and challenges for automotive battery production technologies, Nat. Energy 3 (2018) 290–300, https://doi.org/10.1038/s41560-018-0130-3.

[30] Jan-Hinnerk Schünemann, Modell zur Bewertung der Herstellkosten von Lithiumionenbatteriezellen, 2015.

[31] P. Burggräf, G. Schuh (Eds.), Fabrikplanung, 2nd ed., Springer Vieweg, Berlin, Heidelberg, 2021.

[32] E.C. Bank, Official Interest Rates. https://www.ecb.europa.eu/stats/policy_and_exchange_rates/key_ecb_interest_rates/html/index.de.html, 2023.

[33] Turner and Townsend, International construction market survey 2022 - Continental Europe. https://publications.turnerandtownsend.com/international-construction-market-survey-2022/continental-europe, 2022 (accessed 13 June 2023).

[34] Statistische Bundesamt, Data on Energy Price Trends. https://www.destatis.de/EN/Themes/Economy/Prices/Publications/Downloads-Energy-Price-Trends/energy-price-trends-pdf-5619002.html, 2022.

[35] International Labour Organization, ILOSTAT Data Explorer. https://www.ilo.org/shinyapps/bulkexplorer39/?lang=en&id=LAC_4HRL_ECO_CUR_NB_A, 2023 (accessed 11 June 2023).

[36] Wuxi Lead Intelligent Equipment Co., Ltd, Company Profile. https://www.leadchina.cn/en/about#d1, 2023 (accessed 11 June 2023).

[37] Dürr Systems AG, Electrode Coating. https://www.durr.com/en/products/electromobility-battery/energy-storage/electrode-coating, 2023 (accessed 11 June 2023).

[40] H.H. Heimes, A. Kampker, C. Lienemann, M. Locke, C. Offermanns, Lithium-ion Battery Cell Production Process. https://www.pem.rwth-aachen.de/global/show_document.asp?id=aaaaaaaaabdqbtk, 2019 (accessed 26 June 2023).

[41] European Central Bank, ECB euro reference exchange rate: US dollar (USD). https://www.ecb.europa.eu/stats/policy_and_exchange_rates/euro_reference_exchange_rates/html/eurofxref-graph-usd.de.html, 2023 (accessed 12 June 2023).

[42] A. Jinasena, O.S. Burheim, A.H. Strømman, A flexible model for benchmarking the energy usage of automotive lithium-ion battery cell manufacturing, Batteries 7 (2021) 14, https://doi.org/10.3390/batteries7010014.

[43] Manz AG, Laserschneiden und Lasernotching. https://www.manz.com/de/portfolio/technologien/laserbearbeitung/laserschneiden/, 2023 (accessed 11 June 2023).

[44] TRUMPF SE + Co. KG, Fertigung von Batteriezellen für die Elektromobilität. https://www.trumpf.com/de_DE/loesungen/branchen/automobil/e-mobility/batteriezellen-und-module/, 2023 (accessed 11 June 2023).

[45] Edmund Optics Inc., TRUMPF TruPulse nano gepulste Faserlaser. https://www.edmundoptics.de/f/trumpf-trupulse-nano-pulsed-fiber-lasers/39800/, 2023 (accessed 11 June 2023).

[46] Deutsche Bundesbank, ECB Interest Rates. https://www.bundesbank.de/en/statistics/money-and-capital-markets/interest-rates-and-yields/ecb-interest-rates-626986, 2023.

[47] Department for Energy Security and Net Zero, International industrial energy prices. https://www.gov.uk/government/statistical-data-sets/international-industrial-energy-prices, 2023 (accessed 26 June 2023).

[48] Wirtschaft und Klimaschutz, BMWK - Bundesministerium für, Habeck legt Arbeitspapier zum Industriestrompreis vor. https://www.bmwk.de/Redaktion/DE/Pressemitteilungen/2023/05/20230505-habeck-legt-arbeitspapier-zum-industriestrompreis-vor.html, 2023 (accessed 26 June 2023).

[49] IHS Markit via Statista, Manufacturing labor costs per hour: China, Vietnam, Mexico 2016-2020 | Statista. https://www.statista.com/statistics/744071/manufacturing-labor-costs-per-hour-china-vietnam-mexico/, 2023 (accessed 26 June 2023).

[50] Federal Statistical Office of Switzerland, Labour costs. https://www.bfs.admin.ch/bfs/en/home/statistics/work-income/wages-income-employment-labour-costs/labour-costs.html, 2023 (accessed 26 June 2023).

[51] F. Duffner, L. Mauler, M. Wentker, J. Leker, M. Winter, Large-scale automotive battery cell manufacturing: analyzing strategic and operational effects on manufacturing costs, Int. J. Prod. Econ. 232 (2021), 107982, https://doi.org/10.1016/j.ijpe.2020.107982.